Aalborg Universitet

AALBORG UNIVERSITY
DENMARK

Ultra-Reliable Communications in Failure-Prone Realistic Networks

Gerardino, Guillermo Andrés Pocovi; Lauridsen, Mads; Alvarez, Beatriz Soret; Pedersen, Klaus I.; Mogensen, Preben Elgaard

Published in:
Wireless Communication Systems (ISWCS), 2016 International Symposium on

DOI (link to publication from Publisher):
10.1109/ISWCS.2016.7600939

Publication date:
2016

Document Version
Accepted author manuscript, peer reviewed version

Link to publication from Aalborg University

Citation for published version (APA):
Gerardino, G. A. P., Lauridsen, M., Alvarez, B. S., Pedersen, K. I., & Mogensen, P. E. (2016). Ultra-Reliable Communications in Failure-Prone Realistic Networks. In *Wireless Communication Systems (ISWCS), 2016 International Symposium on* (pp. 414-418). IEEE. https://doi.org/10.1109/ISWCS.2016.7600939

General rights
Copyright and moral rights for the publications made accessible in the public portal are retained by the authors and/or other copyright owners and it is a condition of accessing publications that users recognise and abide by the legal requirements associated with these rights.

- Users may download and print one copy of any publication from the public portal for the purpose of private study or research.
- You may not further distribute the material or use it for any profit-making activity or commercial gain
- You may freely distribute the URL identifying the publication in the public portal -

Take down policy
If you believe that this document breaches copyright please contact us at vbn@aub.aau.dk providing details, and we will remove access to the work immediately and investigate your claim.

Downloaded from vbn.aau.dk on: March 29, 2024

Ultra-Reliable Communications in Failure-Prone Realistic Networks

Guillermo Pocovi[1], Mads Lauridsen[1], Beatriz Soret[2], Klaus I. Pedersen[1,2], Preben Mogensen[1,2]

[1]Department of Electronic Systems, Aalborg University, Denmark,
[2]Nokia - Bell Labs, Aalborg, Denmark
E-mail: gapge@es.aau.dk

***Abstract*—We investigate the potential of different diversity and interference management techniques to achieve the required downlink SINR outage probability for ultra-reliable communications. The evaluation is performed in a realistic network deployment based on site-specific data from a European capital. Micro and macroscopic diversity techniques are proved to be important enablers of ultra-reliable communications. Particularly, it is shown how a 4x4 MIMO scheme with three orders of macroscopic diversity can achieve the required SINR outage performance. Smaller gains are obtained from interference cancellation, since this technique does not increase the diversity order of the desired signal. In addition, failures or malfunction of the cellular infrastructure are analysed. Among different types of failures evaluated, results show that failures spanning over large geographical areas can have a significant negative performance impact when attempting to support high reliability use cases.**

I. Introduction

Ultra-reliable communications over wireless is an active research topic that will open the possibility of novel applications [1]. For some of the use cases, latencies of a few milliseconds must be guaranteed with reliability levels up to 99.999%. The experienced signal to interference-and-noise ratio (SINR) is a metric closely related to the achievable reliability in cellular systems: the higher the SINR, the more feasible it is to achieve low packet error probability and low communication latency.

Studying the potential of different techniques to achieve the required SINR outage probability for ultra-reliable communications is the objective of this paper. In this context, microscopic and macroscopic spatial diversity techniques have shown promising benefits. As an example, the work in [2] evaluates different multiple-input multiple-output (MIMO) antenna configurations to achieve high reliability in a factory environment, whereas [3] analyses the effectiveness of different transmission methods, including microscopic diversity and hybrid automatic repeat request (HARQ) mechanisms. The work in [4], studies the benefit of combined microscopic and macroscopic diversity schemes in different locations of a regular hexagonal network, however without accounting for the multi-user multi-cell interference, which is typically a performance degrading factor. These effects have been included in our previous contribution, where we have identified the required level of diversity and interference management in a 3GPP hexagonal macro network [5].

So far, fading and interference have been the limiting factors of the end-user reliability performance. However, due to the stringent reliability requirements, other sources of instability and error should also be included in the analyses. As an example, malfunction or failure of network components could compromise the performance of the network. The causes of network failures can be commonly classified into power, hardware and software, and can occur at the base stations, aggregation nodes, or at the backhaul links [6], [7]. To the best of our knowledge, the system performance impact of these events on ultra-reliable communications has not been quantified.

In this paper, we aim at identifying the required level of diversity and interference management in order to achieve the required SINR outage probability for ultra-reliable communications. We build on the recent study in [5] with the following additional contributions: (i) Analysis in a realistic network deployment based on site-specific data from a European capital. As compared to regular 3GPP scenarios, the use of site-specific models provides higher degree of realism and practical relevance of the results. (ii) System-level evaluation including the effects of multi-user/multi-cell interference and the increased resource consumption as a consequence of the macroscopic diversity overhead. And (iii) impact of the instability and failure-prone characteristics of real cellular deployments, using a stochastic model for geographically correlated and uncorrelated equipment failures. In order to account for these multiple aspects of realism, the chosen evaluation methodology is system-level Monte-Carlo simulations.

The rest of the paper is organized as follows: Section II describes the considered network scenario. Section III outlines the studied techniques as well as the failure model. The simulation methodology is presented in Section IV. Performance results are shown in Section V, and concluding remarks are given in Section VI.

II. Network layout

A site-specific network layout of an existing LTE macro deployment in a European capital area is reproduced. A three-dimensional (3D) topography map is used for the considered dense urban area [8]. The map contains 3D data of buildings, streets, open squares, parks, etc. Macro cells are placed following a real deployment in the considered area. The macro site antennas are deployed at different heights, taking the local environment characteristics into account in order to have good wide area coverage. The average macro antenna height is 30 meters, using a few degrees of antenna downtilt. The area includes hundreds of macro-sites with 2 and 3 sectors, with an average inter-site distance of 350 meters, covering a geographical area of around 30 km^2. However, the evaluation is limited to the outdoor locations of the 1.2 km^2 segment

depicted in Fig. 1. The outdoor area is mainly represented by streets, avenues and open squares. Hence, the study is relevant for outdoor high reliability use cases, e.g. vehicular communications (V2X) through cellular infrastructure [9].

The radio propagation characteristics are obtained by using state-of-the-art ray-tracing techniques based on the Dominant Path Model (DPM) [10]. This includes the effects of both distance-dependent attenuation and shadowing. The resulting coverage area for each macro cell varies significantly, as the areas shape according to the streets, buildings, among other objects considered in the network model.

III. System model

A set of cells denoted by $\mathcal{N} = \{1, ..., N\}$ are deployed following the network deployment described in Section II. The SINR at the mobile terminal (MT) can be improved in multiple ways. For example, both the serving cell and MT can be equipped with multiple antennas in order to provide increased microscopic diversity. Additionally, various spatially-separated cells can cooperatively serve MTs to provide higher order of macroscopic diversity. As an alternative approach, the received interference can be reduced by applying interference cancellation techniques.

A. SINR model

In order to evaluate the performance of these techniques, we utilize the signal model described in [5]. Each downlink connection between a MT and a cell is represented by a MIMO system with T transmit antennas and R receive antennas. Closed-loop single-stream transmission modes are considered. In a frequency-flat fading case, the R-dimensional received signal $\mathbf{r}_j$ by a user served in cell $j \in \mathcal{N}$ is given as follows,

$$\mathbf{r}_j = \mathbf{H}_j \sqrt{\Omega_j} \mathbf{v}_j s_j + \sum_{i \in \mathcal{N} \setminus j} \mathbf{H}_i \sqrt{\Omega_i} \mathbf{v}_i s_i + \mathbf{n}\,, \tag{1}$$

where $\mathbf{H}_i$ is a RxT matrix whose (m,n)-th element represents the complex channel gain from transmit antenna n at cell i, to receive antenna m; $\mathbf{v}_i$ is the T-dimensional precoding vector used at the i-th cell; Ω_i represents the averaged received power from the i-th cell; s_i represents the transmitted symbol (for simplicity, $\|s_i\| = 1$); and $\mathbf{n}$ is a $Rx1$ zero mean Gaussian vector with variance σ^2 representing the noise power at each receiving antenna. At the receiver, the R received signals are combined by applying a weight vector $\mathbf{w}_j$. The transmitter and receiver weights expressions are given by $\mathbf{v}_j = \mathbf{u}$ and $\mathbf{w}_j = \mathbf{H}_j \mathbf{u}$, where $\mathbf{u}$ is the unitary ($\|\mathbf{u}\| = 1$) eigenvector corresponding to the largest eigenvalue of the $\mathbf{H}_j^H \mathbf{H}_j$ matrix, and $[\cdot]^H$ denotes the Hermitian transpose. This combining method corresponds to maximal-ratio combining (MRC), which aims at maximizing the desired signal power at the receiver. The resulting instantaneous post-detection SINR expression is given by,

$$SINR_j = \frac{\Omega_j \|\mathbf{u}^H \mathbf{H}_j^H \mathbf{H}_j \mathbf{u}\|^2}{\sum_{i \in \mathcal{N} \setminus j} \Omega_i \|\mathbf{u}^H \mathbf{H}_j^H \mathbf{H}_i \mathbf{v}_i\|^2 + \sigma^2 \|\mathbf{u}^H \mathbf{H}_j^H\|^2}\,. \tag{2}$$

For cases where a MT is served with macroscopic diversity, a simple soft-combining approach as known from Universal Mobile Telecommunications System (UMTS) is assumed. The received signal from each macroscopic branch

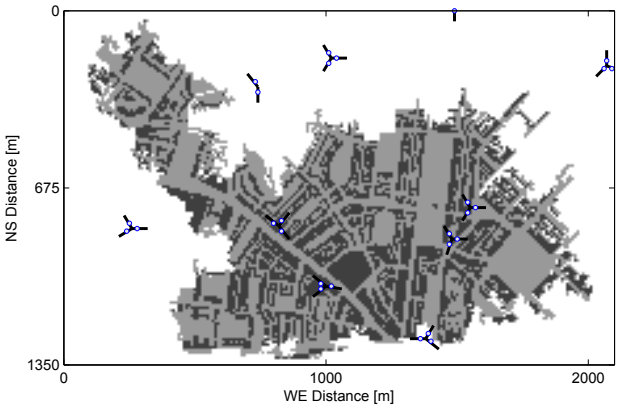


Fig. 1: Illustration of the network layout. The macro cells are marked with blue circles and a line pointing in the direction of the main lobe of the antenna (a.k.a. broadside). Light and dark grey colour denote outdoor and indoor areas, respectively.

is independently detected and combined at the MT [11]. The SINR after combining M ($1 \leq M \leq N$) macro branches is expressed as follows,

$$SINR = \sum_{j=1}^{M} SINR_j\,, \tag{3}$$

where $SINR_j$ is the SINR calculated according to (2), assuming the MT is connected to cell j. The set of cells serving a certain MT is typically referred to as the active set. A *macroscopic diversity window* is applied for the active set selection procedure; i.e. for each MT, the set of serving cells is limited to those whose received power difference is within a certain window, as compared to the strongest cell. Using an appropriate window size, much of the macroscopic diversity gain can be obtained with a reduced resource consumption and less interference generated as compared to the infinite window case [11].

Finally, cases with interference cancellation are also considered. Ideal cancellation of the signal received from the C ($1 \leq C \leq N-1$) strongest interfering cells is assumed. The corresponding SINR expression is similar to (2), with the denominator accounting only for the remaining $N - C - 1$ interferers (we refer to [5] for more details).

B. Network failures

A stochastic model is used to study the impact of network failures as an additional source of degradation of the SINR outage performance. Let $\mathbf{P}$ be a vector composed of N random variables (r.v.) P_1, P_2,..., P_N, where P_n is a Bernoulli distributed r.v. indicating the functional state of cell $n \in \mathcal{N}$. $P_n = 1$ indicates normal operation, and $P_n = 0$ is failure. The probability of failure for cell n is,

$$\mathrm{F}_n = \Pr(P_n = 0) = 1 - \Pr(P_n = 1) \;\; \forall \;\; n \in \mathcal{N}. \tag{4}$$

The geographical characteristics of a potential failure is described in terms of the pairwise correlation, i.e.

$$\rho(m,n) = \frac{\mathrm{cov}(P_n, P_m)}{\sigma_{P_n} \sigma_{P_m}} = \frac{\mathrm{E}[P_n P_m] - \mathrm{E}[P_n]\mathrm{E}[P_m]}{\sigma_{P_n} \sigma_{P_m}} \; \forall m, n \in \mathcal{N} \tag{5}$$

where E[x] and σ_x denote, respectively, the expectation and standard deviation of the r.v. x, and cov(x, y) is the covariance of x and y.

Geographically uncorrelated failures are generally the most common in real networks [6]. Factors such as malfunction of hardware in the cell, buggy software updates, cut of the wired link carrying the data to the core network, etc. can result in localized failures. Correlated failures are less common but not completely absent in real networks. Causes of failure include software upgrades (if performed simultaneously to multiple base stations), hacking of the system (e.g. jamming [12]), natural disasters (storms, earthquakes, etc.), and discharge of batteries after long power outages (especially for small cells with typically small power backup).

We model cases with geographically uncorrelated and correlated failures. The former is among the simplest case as there is independent failure probability at each cell, i.e. $\rho(m, n) = 0$, $m \neq n$. For the case where geographical correlation is present, $\rho(m, n)$ is modelled using an exponential decaying function as follows,

$$\rho(m, n) = \exp\left(\frac{-D_{m,n}}{\mu}\right) \quad \forall \quad n, m \in \mathcal{N}, \tag{6}$$

where $D_{m,n}$ is the distance (in meters) between cells m and n, and μ is the spatial correlation distance. Given these definitions, we build the covariance matrix $\Sigma(\mathbf{P})$ for the set of cells $\mathcal{N}$ and apply methods such as the ones described in [13], [14] to generate samples of binary r.v. with the specified spatial correlation properties.

IV. Simulation methodology

The evaluation is carried out by analysing the downlink SINR distribution with different degrees of micro and macroscopic diversity, and interference management techniques. A snapshot-based simulation approach is applied and the respective assumptions are summarized in Table I. Cells are located as described in Section II and transmitting at full power (full load conditions) at 2.6 GHz carrier frequency. MTs are uniformly distributed in the corresponding area of interest (see Fig. 1). The simulation procedure is as follows: Each MT selects its active set of size M (M corresponds to the macroscopic diversity order) from the set of candidate cells according to the average received power. The set of candidate cells corresponds to those cells in normal operation state and is calculated on every simulation snapshot following the stochastic failure model described in Section III-B. Cells in failing state are assumed to have zero transmit power. Effects of user mobility and handovers are not explicitly included in the simulations. However, the effect of handover hysteresis margin is implicitly modelled in the active set selection algorithm: each MT identifies the strongest received cells that are within a certain *handover window*, as compared to the strongest cell. A serving cell for the MT is then randomly selected from the cells within the handover window. This method models the effect where not all MTs are served by their strongest cell due to the use of handover hysteresis margins in reality.

After the active set selection procedure, the experienced instantaneous post-detection SINR is calculated for each MT following the models in Section III-A. For each snapshot, the fast fading is independent and identically distributed for each transmit-receive antenna pair, following a complex Gaussian distribution (i.e. the envelope is Rayleigh distributed). Additive noise with a power spectral density of −174 dBm/Hz is considered. It is assumed that MTs are assigned with 10 MHz bandwidth, resulting in a noise power of −96 dBm when including a 8 dB noise figure at the MT. In order to emulate the limited feedback capacity of real systems, precoding vector $\mathbf{u}$ is quantized and restricted to the predefined set of codewords used in Long Term Evolution (LTE) [15].

TABLE I: Simulation assumptions

Parameter	**Value**
Network layout	Site-specific network
Macro cell transmit power	46 dBm
Carrier frequency	2.6 GHz
Propagation	Dominant path model [10]
Macro cell antenna configuration	Realistic 3D antenna pattern
MT distribution	Uniformly distributed in outdoor locations
MT antenna configuration	Omnidirectional with 0 dBi gain
Noise power spectral density	-174 dBm/Hz
Noise figure	8 dB
Noise power	-96 dBm @10 MHz
Fast fading	Rayleigh distributed; Uncorrelated among the different antenna branches
Handover window	3 dB
μ, ρ	Uncorrelated failures: $\rho = 0$ Correlated failures: $\rho > 0$, μ = 415 m
SINR outage target	0 dB at the 10^{-5}-th percentile

A large number of snapshots are simulated and the generated SINR samples from all the users are used to form empirical cumulative distribution functions (CDF). In line with [1], the key performance indicator (KPI) is the SINR at the 10^{-5}-th percentile. At this percentile, we consider a 0 dB SINR as an appropriate target to have error-free downlink reception, and therefore fulfil the low latency requirements of ultra-reliability use cases (we refer to [5] for more details).

V. Performance results

Fig. 2 shows the empirical CDF of the SINR distribution with 2x2 and 4x4 microscopic schemes and different orders of macroscopic diversity. For this set of results, all MTs are assumed to have the same macroscopic diversity order equal to M, i.e. no macroscopic diversity window constraint is applied. Normal operation of the network is also assumed. At the 10^{-5}-th percentile, the SINR obtained with 2x2 and 4x4 configurations and no macroscopic diversity is approximately -15 and -7 dB, which is not sufficient for ultra-reliable communications. In contrast, when combined with macroscopic diversity, the diversity order is increased, which results in steeper slopes and significantly better SINR performance. It is observed that $M = 3$ macroscopic links, each with 4x4 MIMO, are required to fulfil the 0 dB SINR requirement. The macroscopic gain comes from the higher received power of the desired signal as well as the additional diversity to combat both fast and slow fading. The soft-combining gain is especially relevant for MTs close to the cell boundaries, which are likely to receive similar power from the M serving cells. Macroscopic diversity also minimizes the negative performance impact of the considered handover hysteresis window, since the probability of not being connected to the strongest cell is reduced.

Fig. 3 summarizes the SINR performance at the 10^{-5}-th percentile with the different diversity configurations, including

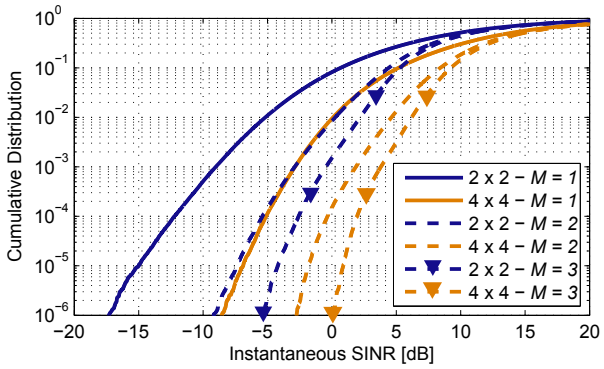


Fig. 2: SINR performance with different levels of macroscopic diversity applied to 2x2 and 4x4 MIMO configurations. M indicates the macroscopic diversity order.

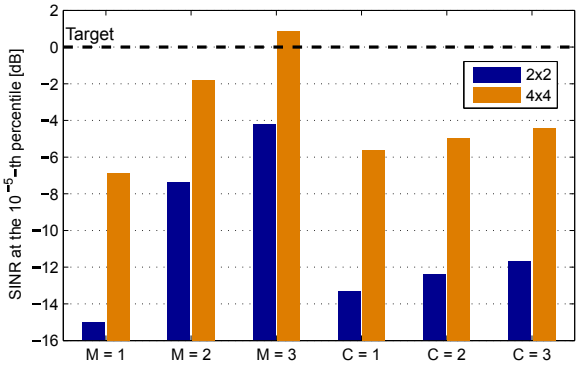


Fig. 3: Achieved SINR at the 10^{-5}-th percentile with different levels of micro- and macroscopic diversity, and interference cancellation. M and C indicate respectively: level of macroscopic diversity and number of interfering signals cancelled.

cases with ideal interference cancellation of the C strongest interferers (assuming $M = 1$ macroscopic diversity order). The 0 dB SINR target is represented with a horizontal dashed line. As previously mentioned, a 4x4 microscopic scheme with $M = 3$ macroscopic links are required to achieve the necessary SINR outage performance in the considered site-specific network, which is one more macroscopic link compared to our previous evaluation in a standard 3GPP macro scenario [5]. The gain obtained by cancelling up to $C = 3$ interferers is 3.4 dB and 2.5 dB for the 2x2 and 4x4 antenna configurations, respectively, which is not sufficient to fulfil the 0 dB SINR outage target. Compared to the spatial diversity techniques, interference cancellation does not increase the slope of the SINR distribution since the diversity order remains the same. The obtained gains of interference cancellation are smaller than reported in the 3GPP macro network [5], as the considered realistic scenario is less interference-limited.

Increasing the diversity by collocating multiple antennas at the transmitter and/or receiver is a radio-resource efficient way to improve the SINR outage performance. A 2x2 MIMO configuration is the most commonly used scheme in LTE, although 4x4 configurations are also allowed in the standard. Practical implementation of macroscopic diversity schemes is more challenging. Among others, tight coordination and low latency communication between cells are required to support the scheme presented in this study. In addition, macroscopic diversity consumes transmission resources for a single user at multiple cells potentially having impact on the system capacity.

It is reasonable to think that when the performance degradation due to increased resource consumption (and interference) exceeds the diversity gain, macroscopic diversity does not provide any benefit to the system performance. To account for this increased resource usage, the *macroscopic diversity overhead* (β) is defined as follows [11],

$$\beta = \sum_{m=1}^{M} m R_m \,, \tag{7}$$

where R_m is the ratio of MTs with macroscopic diversity order equal to m. The overhead is highest for the case when all the MTs are configured with macroscopic diversity order M, whereas it is lower if this technique is only applied to a fraction of the MTs, e.g. by applying a macroscopic diversity window as explained in Section III-A. Taking this overhead into account, Fig. 4 depicts the macroscopic diversity performance with different macroscopic diversity windows. The respective distribution of the macroscopic diversity order for the MTs is written above each group of bars. For each window size, β is calculated according to (7) and subtracted (in dB) from the SINR performance obtained via simulations. We refer to this resulting metric as *compensated SINR*. It is worth mentioning that the objective of this metric is to reflect the cost of applying macroscopic diversity, and not to reflect the actual performance. It is observed that the optimal macroscopic diversity window depends on the configuration of interest. For example, a 4x4 MIMO with $M = 3$ achieves the best performance with a 6 dB macroscopic diversity window, whereas a 2x2 scheme with $M = 3$ would require a larger window, e.g. 10 dB .

The last set of results accounts for malfunctions of the cellular infrastructure. Fig. 5 illustrates the obtained SINR at the 10^{-5}-th percentile when geographically correlated or uncorrelated failures occur with a certain failure probability in the realistic network scenario. For the case of correlated failures, the correlation distance μ is set to 415 meters. This corresponds to a correlation of approximately 0.3 for two cells separated at 500 meter distance. Only the SINR performance with 4x4 and different macroscopic diversity orders is depicted; however, similar trends are also obtained with 2x2 microscopic diversity schemes. It is observed that uncorrelated failures do not result in significant degradation of the performance. In this case, there is sufficient overlapping coverage as it is generally the case for dense urban cellular networks. In the case of correlated failures, there is relatively high impact for all the evaluated configurations since the failures span over large geographical areas in a clustered manner, hence decreasing the probability of having good coverage. The relative performance degradation is more significant for high macroscopic diversity orders, as the additional (weaker) redundant links would typically experience higher pathloss and therefore are more affected by the noise. For example, the 4x4 configuration with three macroscopic links no longer fulfils the required SINR outage performance if the mean failure probability is higher than 0.5%. It is worth to highlight that the interruption time when switching the connectivity from a failing cell to a fully functional cell could potentially be another source of performance degradation that has not been accounted for in this study. Future work must

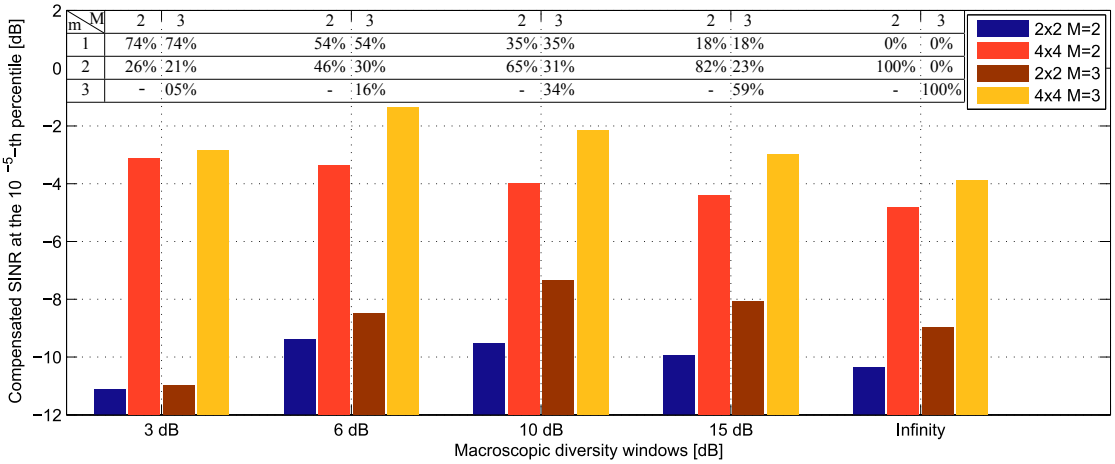


Fig. 4: Compensated SINR at the 10^{-5}-th percentile for several macroscopic diversity windows accounting for the macroscopic diversity overhead. M refers to the maximum allowed macroscopic diversity order. For each configuration, the percentage of users with macroscopic diversity order m is given above each group of bars.

include the validation of our failure model by e.g. analysing real network mean time between failure (MTBF) and mean time to repair (MTTR) statistics.

VI. Conclusion

In this study, we have evaluated the potential of diversity and interference management techniques to achieve very low SINR outage probability as required for ultra-reliable communications. The analysis has been carried out for a realistic site-specific deployment from a big European city. Micro and macroscopic diversity techniques have been shown to be important enablers of ultra-reliable communications. A 4x4 MIMO scheme with three orders of macroscopic diversity is suggested as a feasible configuration to achieve the required SINR outage performance. Mitigating the interference provides complementary benefit, although it does not increase the diversity order of the desired signal. In addition, failures of the cellular network infrastructure have been considered. Different failure probabilities and geographical dimensions have been evaluated. It has been shown that failures spanning over large geographical areas in a correlated manner can have a significant negative impact when attempting to support high reliability use cases.

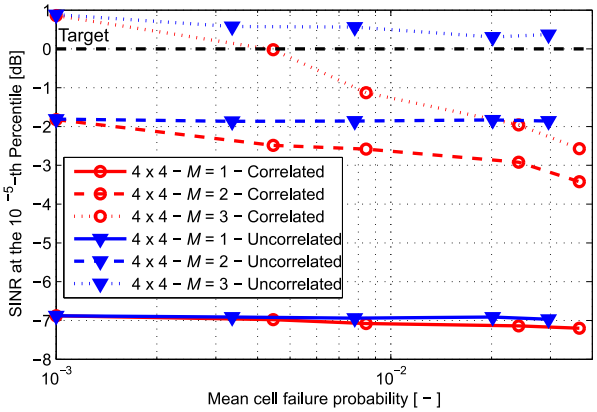


Fig. 5: Achieved SINR at the 10^{-5}-th percentile for different failure types and probabilities. $\mu = 415$ meters.

References

[1] 3GPP TR 38.913 v0.3.0, "Study on scenarios and requirements for next generation access technologies", March 2016.

[2] N. A. Johansson, Y. P. Eric Wang, Erik Eriksson and Martin Hesslear, "Radio access for ultra-reliable and low-latency 5G communications", *IEEE ICC Workshops*, June 2015.

[3] H. Shariatmadari, S. Iraji and R. Jäntti, "Analysis of transmission methods for ultra-reliable communications", *IEEE PIMRC Workshops*, 2015.

[4] F. Kirsten, D. Ohmann, M. Simsek and G. P. Fettweis, "On the utility of macro- and microdiversity for achieving high availability in wireless networks", *IEEE PIMRC*, Sept. 2015.

[5] G. Pocovi, B. Soret, M. Lauridsen, K. I. Pedersen and P. Mogensen, "Signal quality outage analysis for ultra-reliable communications in cellular networks", *IEEE Globecom Workshops*, December 2015.

[6] A. Azarfar, J. F. Frigon and B. Sanso, "Improving the reliability of wireless networks using cognitive radios", *IEEE Communications Surveys & Tutorials*, vol. 14, no. 2, pp. 338-354, 2nd Quarter 2012.

[7] M. Monemian, P. Khadivi and M. Palhang, "Analytical model of failure in LTE networks", *IEEE Malaysia International Conference on Communications (MICC)*, December 2009.

[8] C. Coletti, L. Hu, H. Nguyen, I. Z. Kovacs, B. Vejlgaard, R. Irmer and N. Scully, "Heterogeneous deployment to meet traffic demand in a realistic LTE urban scenario", *IEEE Vehicular Technology Conference*, September 2012.

[9] G. Pocovi, M. Lauridsen, B. Soret, K. I. Pedersen and Preben Mogensen, "Automation for on-road vehicles: use cases and requirements for radio design", *IEEE Vehicular Technology Conference*, Sept. 2015.

[10] R. Wahl, G. Wölfle, P. Wertz and P. Wildbolz, "Dominant path prediction model for urban scenarios", *14th IST Mobile and Wireless Communications Summit*, June 2005.

[11] H. Holma, A. Toskala (editors), "WCDMA for UMTS - radio access for third generation mobile communications", Third edition, Wiley, 2004.

[12] M. Lichtman, J. H. Reed, T. C. Clancy and M. Norton, "Vulnerability of LTE to hostile interference", *IEEE Global Conference on Signal and Information Processing*, December 2013.

[13] A. D. Lunn and S. J. Davies, "A note on generating correlated binary variables", *Biometrika*, vol. 85, no. 2, pp. 487-490, 1998.

[14] J. H. Macke , P. Berens, A. S. Ecker, A. S. Tolias and M. Bethge, "Generating spike trains with specified correlation coefficients", *Neural Computation*, vol. 21, no. 2, pp. 397-423, February 2009.

[15] 3GPP TS 36.211 v12.5.0, "Evolved universal terrestrial radio access (E-UTRA); physical channels and modulation", April 2014.